















Cite this: *CrystEngComm*, 2020, 22, 7095

Novel highly substituted thiophene-based n-type organic semiconductor: structural study, optical anisotropy and molecular control†

Jakub Hagara, ^a Nada Mrkyvkova, ^{*ab} Lucia Feriancová, ^c Martin Putala, ^c Peter Nádaždy, ^a Martin Hodas, ^d Ashin Shaji, ^a Vojtech Nádaždy, ^a Mathias K. Huss-Hansen, ^e Matti Knaapila, ^e Jan Hagenlocher, ^d Nadine Russegger, ^d Matthias Zwadlo, ^d Lena Merten, ^d Michaela Sojková, ^f Martin Hulman, ^f Alina Vlad, ^g Pallavi Pandit, ^h Stephan Roth, ^{hi} Matej Jergel, ^{ab} Eva Majková, ^{ab} Alexander Hinderhofer, ^d Peter Siffalovic ^{ab} and Frank Schreiber ^d

Oligothiophenes and their functionalized derivatives have been shown to be a viable option for high-performance organic electronic devices. The functionalization of oligothiophene-based materials allows further tailoring of their properties for specific applications. We have synthesized a new thiophene-based molecule 1-[5'-(2-naphthyl)-2,2'-bithiophen-5-yl]hexan-1-one (NCOH), and we have studied the optical and structural properties of NCOH thin films. NCOH is a highly substituted member of the oligothiophene family, designed to improve its molecular stacking, where the presence of an electron-withdrawing group enhances its electron transport capabilities. Employing *in situ* and time-resolved grazing-incidence wide-angle X-ray scattering (GIWAXS) measurements, we determined the NCOH thin film crystallographic structure and its evolution starting from the early stages of the film growth. We observed strong optical anisotropy resulting from a highly oriented crystallographic structure. Additionally, we investigated the substrate-induced changes of the molecular orientation utilizing the few-layer MoS₂ with different orientations of the atomic layers. This study, with its primary focus on the fundamentally important n-type molecular semiconductor, contributes to the field of organic-based (opto-)electronics.

Received 10th August 2020,
Accepted 2nd October 2020

DOI: 10.1039/d0ce01171a

rsc.li/crystengcomm

Introduction

Organic π -conjugated semiconducting materials have already found applications in electronic devices, namely organic thin film transistors (OFETs) and organic light emitting diodes (OLEDs).^{1–7} Silicon-based semiconductors offer superior

electronic properties, but the use of organic semiconductors (OSCs) allows tuning of the device properties for more specialized applications like photosensors or chemosensors. Unique features of OSCs such as transparency, flexibility, or stretchability open new possibilities for electronic devices.^{8–11} The functionalization of OSCs allows tailoring of the (opto-) electronic and structural properties required for new types of devices that are not possible with the current silicon-based technology.^{12–15}

Oligothiophenes belong to an extensively studied group of OSCs, mainly for their high charge mobilities, light-emitting properties, relatively simple preparation procedures, and their compatibility with bendable/stretchable substrates.^{16–20} Oligothiophenes can be further modified with a suitable substitution to enhance or alter their electronic properties.^{16,21} For example, substitution with an alkyl chain group allows for better solubility in nonpolar solvents which simplifies the preparation of large-area thin films by solution-based methods.^{22–24} Moreover, end-capping the oligothiophenes with a naphthyl group promotes crystallinity and increases oxidation resistance.²⁵ Introducing the electron-withdrawing groups, one can increase the electron

^a Institute of Physics, Slovak Academy of Sciences, Dúbravská cesta 9, 845 11, Bratislava, Slovakia. E-mail: nada.mrkyvkova@savba.sk; Tel: +421 2 59410 501

^b Center for Advanced Materials Application, Slovak Academy of Sciences, Dúbravská cesta 9, Bratislava 845 11, Slovakia

^c Faculty of Natural Sciences, Comenius University in Bratislava, Ilkovičova 6, 842 15 Bratislava, Slovakia

^d Institute of Applied Physics, University of Tübingen, Auf der Morgenstelle 10, D-72076 Tübingen, Germany

^e Department of Physics, Technical University of Denmark, Kgs. Lyngby 2800, Denmark

^f Institute of Electrical Engineering, Slovak Academy of Sciences, Dúbravská cesta 9, 845 11 Bratislava, Slovakia

^g Synchrotron SOLEIL, L'Orme des Merisiers, 91190 Saint-Aubin, France

^h Photon Science, Deutsches Elektronen-Synchrotron (DESY), Hamburg 22607, Germany

ⁱ Department of Fibre and Polymer Technology, KTH Royal Institute of Technology, Teknikringen 56-58, SE-100 44 Stockholm, Sweden

† Electronic supplementary information (ESI) available. See DOI: 10.1039/d0ce01171a

affinity of the molecule, achieving an n-type organic semiconductor.^{26–29} However, adding the substitution groups can significantly modify the structure of the thin film and influence the optical and electronic properties of the device. Hence, it is imperative to study the molecular packing and structural features of thiophene-based thin layers and their dependence on the underlying substrate.

We have chosen a promising candidate of oligothiophenes compounds, namely 1-[5'-(2-naphthyl)-2,2'-bithiophen-5-yl] hexan-1-one (NCOH) that shows appealing characteristics for organic-based (opto)-electronic applications. NCOH was selected based on previous research of thiophene-based OSCs functionalized with naphthalene core.³⁰ The NCOH molecule contains a naphthyl group at one end of the molecular chain (see Scheme 1 below) to enhance the molecular ordering, as well as its air stability.^{20,31} The other end of the thiophene chain is capped with an electron-withdrawing keto group (C=O) to support electron mobility and promote the n-type conductivity. Additionally, the compound is synthesized with pentyl (–C₅H₁₁) group which improves the solubility of the NCOH molecules.^{22,23,32} What is more, the alkyl spacer makes the NCOH molecule more flexible as compared to its symmetric analog with two naphthyl endgroups.²⁵

In this paper, we exploit molecular orientation, crystallographic structure, and optical anisotropy of NCOH molecules grown on a silicon substrate and few-layer molybdenum disulfide (MoS₂). It is known that rod-like molecules, such as NCOH, can usually adopt distinct orientations depending on the interaction strength with the underlying substrate.³³ In the case of weakly interacting substrates (inert/oxidized surfaces) where the intermolecular π – π interactions prevail over the interactions with substrate, molecules adopt the standing-up orientation, *i.e.*, with their longer molecular axis perpendicular to the substrate surface.^{34–37} On the other hand, a lying-down orientation of molecules is observed for strongly interacting substrates such as metals or two-dimensional materials.^{19,35,38–44} We have chosen several substrates to study the crystallographic structure of NCOH that depends on a particular molecular orientation – Si substrate with a native oxide layer and two types of few-layer MoS₂ substrates with mutually perpendicular alignment of atomic layers.

Experimental section

Scheme 1 shows the synthesis of NCOH. The bromobithienyl precursor **1** was synthesized by an electrophilic bromination of hexanoylbithiophene **2** with *N*-bromosuccinimide (NBS).

The target compound NCOH was prepared by Suzuki cross-coupling reaction of **1** with 2-naphthylboronic acid pinacol ester in 81% yield.

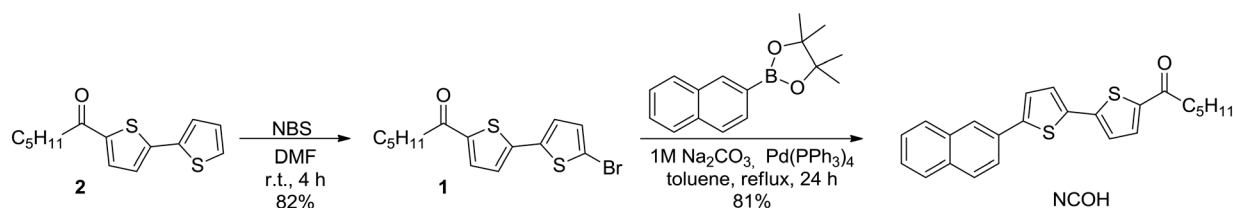
The NCOH was characterized by nuclear magnetic resonance (NMR) spectroscopy and high-resolution mass spectrometry (HRMS) to confirm the molecular structure of the newly synthesized NCOH molecule. A more detailed description of NCOH and bromobithienyl precursor synthesis and the characterization results can be found in the first section of ESI† (Fig. S1–S4).

The n-type properties of the organic semiconductor can be described as preferential injection of the electrons from the metal electrode into the semiconductor. In other words, the n-type organic semiconductor must have a low lying LUMO level (ideally between –3 eV and –4 eV), which corresponds to high electron affinity.^{45,46} Functionalization of the conjugated backbone with electron-withdrawing groups (such as: –NO₂, –C=O, –N=O, –C≡N₂...) decrease the electron density from the π -conjugated system. Such a decrease in electron density leads to an increased electron affinity of the semiconducting material.⁴⁵ In our case, the carbonyl group (C=O) withdraws electron from the π -conjugated core of NCOH molecule to increase electron affinity, leading to LUMO level energy of (–3.2 ± 0.1) eV as determined by EIS (see Fig. S5 in the ESI†).

Few-layer MoS₂ substrates were prepared by magnetron sputtering of molybdenum layers onto 0001 Al₂O₃ substrates. Mo films were subsequently sulfurized in vapors at 800 °C in the inert atmosphere of N₂.⁴⁷ The thickness of the Mo layer determines the orientation of the MoS₂ atomic layers.³⁷ The MoS₂ characterization using the GIWAXS method showed a high degree of film crystallinity and no residual Mo grains.

NCOH thin films were grown by the organic molecular beam deposition (OMBD), *i.e.*, a thermal evaporation method, commonly used for the preparation of thin organic films.^{35,48} We used a custom-built vacuum chamber equipped with a 360° cylindrical beryllium window compatible with *in situ* X-ray diffraction measurements.⁴⁹ NCOH molecules in a powder form were heated to 135 °C and evaporated onto a substrate. A constant deposition rate of ~1.5 Å min^{–1}, monitored by a quartz crystal microbalance in real-time, was maintained during the whole thin-film growth. Before NCOH deposition, the substrate was annealed at 320 °C to remove possible contaminations and subsequently cooled down to a stable temperature of 50 °C. The base pressure inside the vacuum chamber was below 4 × 10^{–8} mbar.

The grazing-incidence wide-angle X-ray scattering (GIWAXS) measurements were performed at SOLEIL (Paris,



Scheme 1 Synthesis of NCOH oligomer.

France) on beamline SIXS and at DESY (Hamburg, Germany) on beamline P03. The energy of the X-ray beam was 12 keV and 11.6 keV at SOLEIL and DESY, respectively. The intensity of the beam was attenuated to 10^{10} photons per s, to prevent X-ray induced photodegradation of the molecules on the sample surface. The angle of incidence (α_i) was set to 0.2° for all measurements. GIWAXS patterns were measured using the XPAD 3.2. single-photon counting 2D detector (SOLEIL) and Pilatus 300 K (DESY). The sample-to-detector (SDD) distance was 218 mm for Si-XPAD and 148 mm for Pilatus 300 K.

Variable angle spectroscopic ellipsometry for NCOH thin film on Si substrate was measured in the reflection geometry, using the spectroscopic ellipsometer J.A. Woollam M-2000 (J. A. Woollam, USA). Ellipsometric measurements were performed in a wavelength range of 245–1700 nm, at the angles of incidence varied between 50° and 70° with a step of 5° .

The thin film topography was measured using the MultiMode8 (Bruker, USA) AFM in a PeakForce mode using the ScanAsyst-Air tips (Bruker, USA). The resolution of the AFM scans was 512×512 pixels.

Results and discussion

NCOH, in the powder form, was thermally evaporated on a Si substrate (with a native SiO_2 layer), creating a thin layer of 15 nm. To investigate the structure of the NCOH thin films, we employed grazing-incidence wide-angle X-ray scattering (GIWAXS). The observed Bragg reflections in the GIWAXS data (Fig. 1) indicate a good structural order of the NCOH film. The diffraction peaks were visible for arbitrary in-plane orientation of the sample, which suggests an isotropic in-plane crystallographic structure also termed as a fiber-like texture on the Si substrate. The isotropic scattering rings originate from the vacuum chambers beryllium window.

The most intense peak at $q_z \sim 0.32 \text{ \AA}^{-1}$ results from the (001) planes of the monoclinic lattice (see further) stacked in the direction perpendicular to the substrate plane. The

spacing of (001) planes along the reciprocal lattice c^* -direction is $d_{001} = (19.7 \pm 0.4) \text{ \AA}$. Taking into account the length of the NCOH molecule ($\sim 19 \text{ \AA}$), we can assume that the molecules are oriented in a standing-up manner with respect to the substrate. Apart from the 001 Bragg peak, diffraction peaks with non-zero h and k Miller indices are visible as well. These peaks originate from the (110), (111), (201), and (202) lattice planes and their sharpness indicates good packing both in-plane as well as out-of-plane.

All measured Bragg reflections (001, 110, 111, 201, and 202) were utilized for the determination of the thin film unit cell parameters a , b , c , α , β , and γ . We fitted the intensity profiles of the diffraction peaks with a Gaussian function in both, q_{xy} and q_z directions, obtaining their reciprocal space positions. Employing the genetic algorithm as the fitting procedure,⁴⁴ the unit cell parameters were calculated. We found that NCOH molecules in a thin film are arranged in a monoclinic structure (space group $P2_1/m$) with the unit cell parameters: $a = (8.4 \pm 0.1) \text{ \AA}$, $b = (6.0 \pm 0.1) \text{ \AA}$, $c = (21.1 \pm 0.5) \text{ \AA}$, and $\beta = (99.6 \pm 0.3)^\circ$, where the given errors include the error from the genetic algorithm calculations and the error induced by the broad sample area probed by the X-rays ($\sim 1 \text{ mm}^2$). The obtained unit cell parameters were subsequently used to calculate the peak positions, as indicated by the black crosses in Fig. 1. The calculated peak positions are in good agreement with the measured Bragg reflections, justifying the obtained values of the unit cell parameters.

In addition, we monitored real-time *in situ* GIWAXS to study the evolution of the unit cell during the NCOH deposition. Similarly to the post-growth calculations, a fit with genetic algorithm was used to determine the unit cell parameters from the measured Bragg reflections. Fig. 2 shows the dependence of the unit parameters on the NCOH layer thickness. We note that the data could be reliably fitted starting from a film thickness of $\sim 3 \text{ nm}$ (~ 1.5 monolayers), when clear diffraction peaks appear. The obtained data show a significant change in the c -parameter, while a , b , and β do not vary substantially during the growth. We observe a reduction of the c -parameter with increasing NCOH layer thickness. A similar evolution of the out-of-plane lattice spacing was reported by Hayakawa *et al.* in ref. 50 for quaterylene growth on Si substrate (we note that in our case, the out-of-plane lattice spacing d_{001} and c -parameter evolve in the same manner, as β was found to be constant during the growth). A change in the c -parameter leads to the unit cell volume decrease by almost 12% for the final film thickness, compared to the initial stages of the deposition. Contraction of the unit cell suggests a reorientation of NCOH molecules inside the unit cell, which appears as a result of the intrinsic stress commonly observed during thin film preparation.^{37,50–52}

We further investigated the morphology of the molecular layers by atomic force microscopy (AFM). Fig. 3 shows the typical AFM images of NCOH films with different thicknesses on the Si substrate. We observed a uniform molecular coverage of the substrate and the Stranski–Krastanov growth

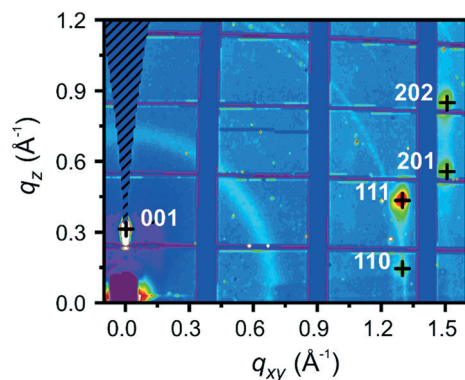


Fig. 1 Reciprocal space map (GIWAXS pattern) of 15 nm thick NCOH thin film on Si substrate (intensity increasing from blue to white). Black crosses indicate the Bragg peak positions calculated from experimentally determined unit cell parameters.

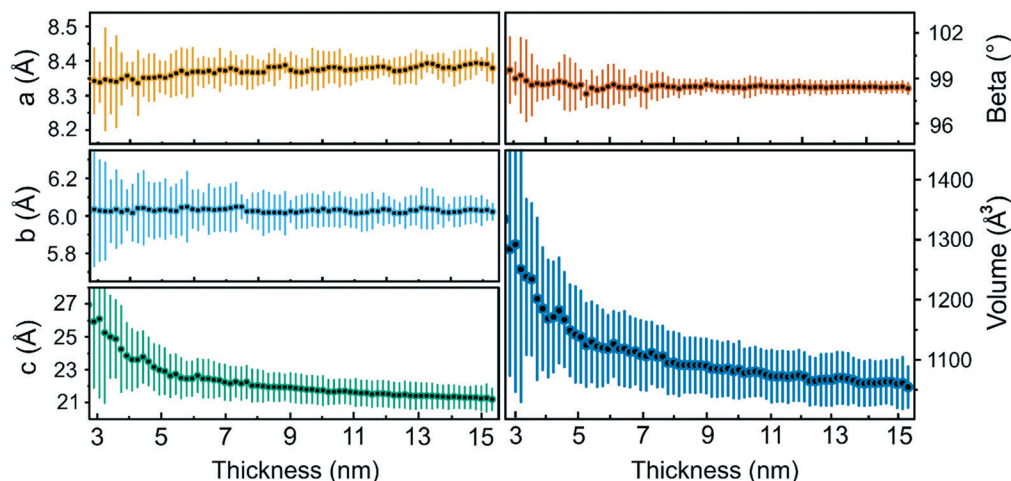


Fig. 2 Thickness dependence of the unit cell parameters a , b , c , and β , together with unit cell volume evolution during the NCOH deposition on Si substrate.

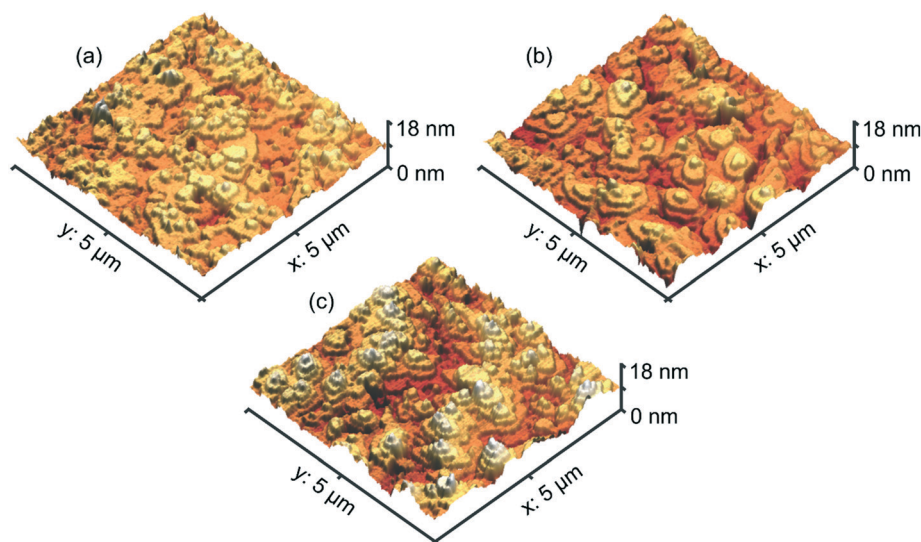


Fig. 3 AFM images of (a) 15 nm, (b) 20 nm, (c) 25 nm thick NCOH thin films on Si substrate.

mode (layer-plus-island)^{34,53} was identified. Here, the bottom layers are fully closed, while the last few layers are not entirely connected, thus creating spatially separated islands. This growth mode is not uncommon for molecular growth on Si substrates, forming so-called wedding-cake-like structures.^{35,50,54,55} The upper layers form planar terraces that are separated from each other by a uniform step of ~ 2 nm (see Fig. S7 in the ESI†). This monomolecular step is consistent with lattice spacing d_{001} , calculated from the GIWAXS pattern.

Furthermore, we studied the optical response of the NCOH thin film on Si substrate. It is well known that molecular anisotropy has a direct influence on the physical properties of the thin film. The optical properties strongly depend on the orientation of the molecules with respect to the direction of incoming light, while the molecular packing and π - π interactions of neighboring molecules influence the

electronic properties of organic films. Similar to many commonly used π -conjugated organic semiconductors, NCOH molecules have a rod-like structure. Consequently, we expected strong optical anisotropy depending on the molecular orientation. Fig. 4 shows the extinction coefficient components in the directions perpendicular (k_z) and parallel (k_{xy}) to the substrate surface. The extinction coefficient was determined by variable angle spectroscopic ellipsometry (VASE). Details concerning the k_{xy} and k_z calculations can be found in ref. 56. The extinction coefficient shows an absorption increase at $E = 2.75$ eV (see Fig. 4), which can be assigned to the width of the HOMO–LUMO bandgap. For the standing-up molecules on Si substrate, we observed a dominant k_z component and only a weak absorption peak for the k_{xy} component. This suggests that the transition dipole moment is oriented parallel to the long molecular axis of NCOH. In other words, the orientation of the NCOH

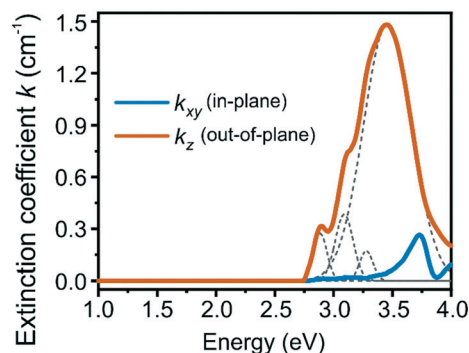


Fig. 4 Extinction coefficient determined from UV-VIS-NIR ellipsometry measured on 23 nm thick NCOH film on Si substrate. The deconvolution of the k_z coefficient into individual peaks is shown.

molecules can be derived directly from the ellipsometry measurements since the magnitude of the extinction coefficients is given by the relative orientation of the molecular transition dipole moment (which, in our case, is oriented along the long molecular axis) and the incident electric field direction. Additionally, the k_z component shows four significant absorption peaks with an equidistant energy spacing of $\Delta E = 0.2 \pm 0.01$ eV. These peaks can be assigned to different vibronic states of the electron $S^0 \rightarrow S^1$ transitions for the NCOH molecule.

In the following paragraph, we will discuss the effect of the underlying substrate on the NCOH molecular orientation. To do so, we employ few-layer molybdenum disulfide (MoS_2) underlayers with different alignments of the atomic layers. In particular, we used MoS_2 substrates with either horizontal or vertical orientation of the atomic layers with respect to the substrate surface.^{47,57} The orientation of MoS_2 layers subsequently influences the orientation of small organic molecules deposited on MoS_2 surface.³⁷

Fig. 5 shows the GIWAXS reciprocal maps of 15 nm thick NCOH film grown on MoS_2 underlayers with two distinct orientations of the atomic layer. The orientation of MoS_2 layers can be determined from the position of the intense

002 diffraction at $q \sim 1 \text{ \AA}^{-1}$. For the vertically aligned MoS_2 layers, Bragg reflection is in the in-plane direction, *i.e.* along q_{xy} , as the unit cell c -parameter of MoS_2 is oriented parallel to the substrate plane (see Fig. 5a). In contrast, the 002 diffraction is in the out-of-plane direction for horizontally aligned MoS_2 layers (see Fig. 5b). We observed that the NCOH molecules deposited on top of the vertically aligned MoS_2 layer are oriented in the standing-up configuration. Their molecular orientation is the same as on the Si substrate shown earlier. This is consistent with the fact that the vertically aligned MoS_2 surface is oxidized due to the presence of chemically active dangling bonds.³⁷ Its surface is thus amorphous, similar to the Si surface with native oxide. The lack of diffraction peaks (other than 001 in Fig. 5a) from the NCOH thin layer suggests a worse in-plane ordering on MoS_2 compared to the Si substrate. This can be attributed mainly to a higher surface roughness of the MoS_2 layer, which is of the order of several nanometers³⁷ (surface roughness of Si surface is ~ 0.3 nm). The vertically aligned MoS_2 layer consists of domains with vertically oriented atomic planes that are randomly oriented in the plane of the sample surface. The NCOH thin film replicates the random in-plane crystalline orientation, causing a very low intensity for crystal planes scattering in the in-plane direction.

In contrast, when NCOH molecules are deposited onto a horizontally aligned MoS_2 layer, they adopt a lying-down orientation, see Fig. 5b. The lying-down molecular orientation results from a stronger interaction between NCOH molecules and horizontally aligned MoS_2 layers, when comparing with the vertically oriented MoS_2 layers. The different strengths of the interaction result from different surface energies of the two MoS_2 atomic orientations (for more details see ref. 37). Similarly, as in the case of vertically aligned MoS_2 layers, only the 001 diffraction from NCOH is visible due to higher MoS_2 roughness (vertically and horizontally aligned MoS_2 underlayers showed similar roughness). It has been shown that the in-plane molecular ordering can be improved when the molecules are deposited on two-dimensional substrates, *e.g.*, graphene or MoS_2 monolayer.^{44,58}

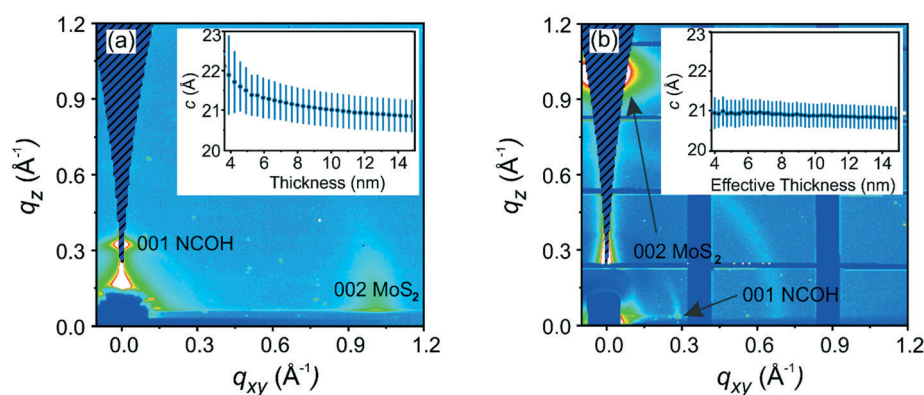


Fig. 5 Reciprocal space map of 15 nm thick NCOH film deposited on a few-layer MoS_2 substrate with (a) vertical and (b) horizontal alignment. The intensity increases from blue to white. The insets show the calculated evolution of the crystallographic c -parameter with increasing NCOH thickness.

From the measured GIWAXS patterns, it was not possible to determine the full set of unit cell parameters because of an insufficient number of detected diffractions. However, the approximate *c*-axis length and its evolution with NCOH growth can be determined from the 001 diffraction peak position. Based on the previous genetic algorithm calculation of NCOH structure on the Si substrate, we did not expect any significant changes in other unit cell parameters during the molecular growth. The *c*-parameter evolution with NCOH film thickness is shown in the insets of Fig. 5. For NCOH grown on the vertically aligned MoS₂ layer, we observed a similar decrease of the *c*-parameter as for the thin film grown on the Si substrate. The similar evolution of the *c*-parameter is not surprising, as in both cases, the molecules interact with amorphous oxidized surfaces. On the other hand, for NCOH grown on a horizontally aligned MoS₂, we did not observe any significant change of the *c*-parameter. It seems that in this case, the interaction between the molecules and the substrate allows the formation of a stress-free film. The stress-free layer does not influence the length of the *c*-axis. We note that we use the term “effective thickness” for the lying-down molecular layer, as the molecules do not form closed layers but rather separated islands on horizontally aligned MoS₂ (see Fig. S8 in the ESI†). For the unclosed layers, the layer thickness is thus hard to define. The effective thickness is related to the total amount of molecules deposited on the substrate, which is the same for both MoS₂ layers, regardless of the thin film morphology. Using the effective thickness even for the unclosed layers, enables direct comparison of *c*-parameter for the lying-down and standing-up molecules.

Conclusions

In conclusion, we have studied the molecular orientation, crystallographic structure, morphology, and optical properties of NCOH thin film. We found that NCOH forms crystals when thermally evaporated on the underlying Si and few-layer MoS₂ substrates. GIWAXS measurements showed that the molecules grow in a standing-up configuration on the oxidized surfaces (Si and vertically aligned MoS₂ layers). The molecules grew in a mode similar to Stranski–Krastanov, where the initial layers were fully closed, gradually being arranged into the so-called wedding-cake structure at the top of the film. Consistently with the GIWAXS results, the ellipsometry measurements confirmed the molecular orientation on Si substrate, showing pronounced absorption spectra for the out-of-plane component of the extinction coefficient. On the other hand, a lying-down molecular orientation was observed for the strongly interacting horizontally aligned MoS₂ layers. Furthermore, we have determined the crystallographic structure of the NCOH thin film on Si substrate and its evolution with film thickness. The reduction of the *c*-parameter with increasing layer thickness for the standing-up molecular orientation was attributed to the continuous tilt of the long molecular axis

within the unit cell. For the lying-down molecules, we did not observe any significant change of the *c*-parameter during the growth.

Conflicts of interest

The authors declare no conflict of interest.

Acknowledgements

We acknowledge the financial support of the projects APVV-19-0365, APVV-18-0480, APVV-17-0352, APVV-17-0560, APVV-17-0501, APVV-16-0319, APVV-15-0641, APVV-15-0693, SK-CN-RD-18-0006, APVV-14-0745, VEGA 2/0092/18, VEGA 2/0149/17, VEGA 1/0595/17, ITMS 26210120023, 26230120002, 26210120002, 26220220170, DAAD/SAV grant, and the funding by the DFG. This work was performed during the implementation of the project Building-up Centre for Advanced Materials Application of the Slovak Academy of Sciences, ITMS project code 313021T081, supported by the Research & Innovation Operational Programme funded by the ERDF. We further acknowledge the Alexander von Humboldt foundation for the financial support of M. Hodas. M. K. Huss-Hansen thanks the Danish Agency for Science, Technology, and Innovation for funding the instrument center DanScatt. Furthermore, we would like to acknowledge the support of the SixS team.

References

- 1 S. Vasimalla, N. V. V. Subbarao and P. K. Iyer, Low Voltage, Low Cost, Flexible and Balanced Ambipolar OFETs Based on Br₂PTCDI-C18/CuPc Fabricated on an Al Foil Gate Substrate with Good Ambient Stability, *J. Mater. Chem. C*, 2016, **4**(29), 7102–7109, DOI: 10.1039/C6TC02315K.
- 2 Y. Huang, H. Chen, J. Yang, W. Tian and W. Wang, 3D-Printed OFETs of the 1,4-Bis(3-Phenylquinoxalin-2-Yl) Benzene-Based Polymer Semiconductors, *Polym. Chem.*, 2017, **8**(33), 4878–4886, DOI: 10.1039/C7PY00810D.
- 3 T. Minami, T. Sato, T. Minamiki, K. Fukuda, D. Kumaki and S. Tokito, A Novel OFET-Based Biosensor for the Selective and Sensitive Detection of Lactate Levels, *Biosens. Bioelectron.*, 2015, **74**, 45–48, DOI: 10.1016/j.bios.2015.06.002.
- 4 S. G. Surya, S. S. Nagarkar, S. K. Ghosh, P. Sonar and V. Ramgopal Rao, OFET Based Explosive Sensors Using Diketopyrrolopyrrole and Metal Organic Framework Composite Active Channel Material, *Sens. Actuators, B*, 2016, **223**, 114–122, DOI: 10.1016/j.snb.2015.09.076.
- 5 G. Li, Y. Zhao, J. Li, J. Cao, J. Zhu, X. W. Sun and Q. Zhang, Synthesis, Characterization, Physical Properties, and OLED Application of Single BN-Fused Perylene Diimide, *J. Org. Chem.*, 2015, **80**(1), 196–203, DOI: 10.1021/jo502296z.
- 6 S. Krotkus, D. Kasemann, S. Lenk, K. Leo and S. Reineke, Adjustable White-Light Emission from a Photo-Structured Micro-OLED Array, *Light: Sci. Appl.*, 2016, **5**(7), e16121–e16121, DOI: 10.1038/lsa.2016.121.

- 7 J. Yu, X. Yu, L. Zhang and H. Zeng, Ammonia Gas Sensor Based on pentacene Organic Field-Effect Transistor, *Sens. Actuators, B*, 2012, **173**, 133–138, DOI: 10.1016/j.snb.2012.06.060.
- 8 Y. Yuan, G. Giri, A. L. Ayzner, A. P. Zoombelt, S. C. B. Mannsfeld, J. Chen, D. Nordlund, M. F. Toney, J. Huang and Z. Bao, Ultra-High Mobility Transparent Organic Thin Film Transistors Grown by an off-Centre Spin-Coating Method, *Nat. Commun.*, 2014, **5**(1), 3005, DOI: 10.1038/ncomms4005.
- 9 L. Basiricò, P. Cosseddu, B. Fraboni and A. Bonfiglio, Inkjet Printing of Transparent, Flexible, Organic Transistors, *Thin Solid Films*, 2011, **520**(4), 1291–1294, DOI: 10.1016/j.tsf.2011.04.188.
- 10 S. K. Gupta, P. Jha, A. Singh, M. M. Chehimi and D. K. Aswal, Flexible Organic Semiconductor Thin Films, *J. Mater. Chem. C*, 2015, **3**(33), 8468–8479, DOI: 10.1039/C5TC00901D.
- 11 A. Chortos, J. Lim, J. W. F. To, M. Vosgueritchian, T. J. Dussault, T.-H. Kim, S. Hwang and Z. Bao, Highly Stretchable Transistors Using a Microcracked Organic Semiconductor, *Adv. Mater.*, 2014, **26**(25), 4253–4259, DOI: 10.1002/adma.201305462.
- 12 J. T. E. Quinn, J. Zhu, X. Li, J. Wang and Y. Li, Recent Progress in the Development of N-Type Organic Semiconductors for Organic Field Effect Transistors, *J. Mater. Chem. C*, 2017, **5**(34), 8654–8681, DOI: 10.1039/C7TC01680H.
- 13 L. Hahn, A. Hermannsdorfer, B. Günther, T. Wesp, B. Bühler, U. Zschieschang, H. Wadepohl, H. Klauk and L. H. Gade, (Oligo-)Thiophene Functionalized Tetraazaperopyrenes: Donor–Acceptor Dyes and Ambipolar Organic Semiconductors, *J. Org. Chem.*, 2017, **82**(23), 12492–12502, DOI: 10.1021/acs.joc.7b02286.
- 14 R. Oshi, S. Abdalla and M. Springborg, The Impact of Functionalization of Organic Semiconductors by Electron Donating Groups on the Reorganization Energy, *Eur. Phys. J. D*, 2019, **73**(6), 124, DOI: 10.1140/epjd/e2019-100020-1.
- 15 J. E. Anthony, Functionalized Acenes and Heteroacenes for Organic Electronics, *Chem. Rev.*, 2006, **106**(12), 5028–5048, DOI: 10.1021/cr050966z.
- 16 M. Melucci, L. Favaretto, C. Bettini and M. Gazzano, Liquid-Crystalline Rigid-Core Semiconductor Oligothiophenes: Influence of Molecular Structure on Phase Behaviour and Thin-Film Properties, *Chem. – Eur. J.*, 2007, **13**, 10046–10054, DOI: 10.1002/chem.200701368.
- 17 L. Zhang, N. S. Colella, B. P. Cherniawski, S. C. B. Mannsfeld and A. L. Briseno, Oligothiophene Semiconductors: Synthesis, Characterization, and Applications for Organic Devices, *ACS Appl. Mater. Interfaces*, 2014, **6**(8), 5327–5343, DOI: 10.1021/am4060468.
- 18 X. Yang, L. Wang, C. Wang, W. Long and Z. Shuai, Influences of Crystal Structures and Molecular Sizes on the Charge Mobility of Organic Semiconductors: Oligothiophenes, *Chem. Mater.*, 2008, **20**(9), 3205–3211, DOI: 10.1021/cm8002172.
- 19 M. K. Huss-Hansen, M. Hodas, N. Mrkyvkova, J. Hagara, B. B. E. Jensen, A. Osadnik, A. Lützen, E. Majková, P. Siffalovic and F. Schreiber, *et al.*, Surface-Controlled Crystal Alignment of Naphthyl End-Capped Oligothiophene on Graphene: Thin-Film Growth Studied by in Situ X-Ray Diffraction, *Langmuir*, 2020, **36**(8), 1898–1906, DOI: 10.1021/acs.langmuir.9b03467.
- 20 H. K. Tian, J. W. Shi, D. H. Yan, L. X. Wang, Y. H. Geng and F. S. Wang, Naphthyl End-Capped Quarterthiophene: A Simple Organic Semiconductor with High Mobility and Air Stability, *Adv. Mater.*, 2006, **18**(16), 2149–2152, DOI: 10.1002/adma.200600178.
- 21 A. Gupta, A. Ali, T. B. Singh, A. Bilic, U. Bach and R. A. Evans, Molecular Engineering for Panchromatic Absorbing Oligothiophene Donor– π –Acceptor Organic Semiconductors, *Tetrahedron*, 2012, **68**(46), 9440–9447, DOI: 10.1016/j.tet.2012.09.009.
- 22 H. H. Fong, V. A. Pozdin, A. Amassian, G. G. Malliaras, D.-M. Smilgies, M. He, S. Gasper, F. Zhang and M. Sorensen, Tetrathienoacene Copolymers As High Mobility, Soluble Organic Semiconductors, *J. Am. Chem. Soc.*, 2008, **130**(40), 13202–13203, DOI: 10.1021/ja804872x.
- 23 S. Inoue, H. Minemawari, J. Tsutsumi, M. Chikamatsu, T. Yamada, S. Horiuchi, M. Tanaka, R. Kumai, M. Yoneya and T. Hasegawa, Effects of Substituted Alkyl Chain Length on Solution-Processable Layered Organic Semiconductor Crystals, *Chem. Mater.*, 2015, **27**(11), 3809–3812, DOI: 10.1021/acs.chemmater.5b00810.
- 24 A.-L. Deman, J. Tardy, Y. Nicolas, P. Blanchard and J. Roncali, Structural Effects on the Characteristics of Organic Field Effect Transistors Based on New Oligothiophene Derivatives, *Synth. Met.*, 2004, **146**(3), 365–371, DOI: 10.1016/j.synthmet.2004.08.015.
- 25 H. K. Tian, J. W. Shi, B. He, N. H. Hu, S. Q. Dong, D. H. Yan, J. P. Zhang, Y. H. Geng and F. S. Wang, Naphthyl and Thionaphthyl End-Capped Oligothiophenes as Organic Semiconductors: Effect of Chain Length and End-Capping Groups, *Adv. Funct. Mater.*, 2007, **17**(12), 1940–1951, DOI: 10.1002/adfm.200706198.
- 26 A. Naibi Lakshminarayana, A. Ong and C. Chi, Modification of Acenes for N-Channel OFET Materials, *J. Mater. Chem. C*, 2018, **6**(14), 3551–3563, DOI: 10.1039/C8TC00146D.
- 27 M. Melucci, M. Zambianchi, L. Favaretto, M. Gazzano, A. Zanelli, M. Monari, R. Capelli, S. Troisi, S. Toffanin and M. Muccini, Thienopyrrolyl Dione End-Capped Oligothiophene Ambipolar Semiconductors for Thin Film- and Light Emitting Transistors, *Chem. Commun.*, 2011, **47**(43), 11840–11842, DOI: 10.1039/c1cc14179a.
- 28 K. Tsukamoto, K. Takagi, S. Nagano, M. Hara, Y. Ie, K. Osakada and D. Takeuchi, π -Extension of Electron-Accepting Dithiarubicene with a Cyano-Substituted Electron-Withdrawing Group and Application in Air-Stable n-Channel Organic Field Effect Transistors, *J. Mater. Chem. C*, 2019, **7**(40), 12610–12618, DOI: 10.1039/C9TC04325J.
- 29 S. W. Yun, J. H. Kim, S. Shin, H. Yang, B.-K. An, L. Yang and S. Y. Park, High-Performance n-Type Organic Semiconductors: Incorporating Specific Electron-Withdrawing Motifs to Achieve Tight Molecular Stacking and Optimized Energy Levels, *Adv. Mater.*, 2012, **24**(7), 911–915, DOI: 10.1002/adma.201103978.

- 30 J. Filo, R. Mišćák, M. Cigán, M. Weis, J. Jakabovič, K. Gmucová, M. Pavúk, E. Dobročka and M. Putala, Oligothiophenes with the Naphthalene Core for Organic Thin-Film Transistors: Variation in Positions of Bithiophenyl Attachment to the Naphthalene, *Synth. Met.*, 2015, **202**, 73–81, DOI: 10.1016/j.synthmet.2015.01.020.
- 31 H. Nagashima, M. Saito, H. Nakamura, T. Yasuda and T. Tsutsui, Organic Field-Effect Transistors Based on Naphthyl End-Capped Divinylbenzene: Performance, Stability and Molecular Packing, *Org. Electron.*, 2010, **11**(4), 658–663, DOI: 10.1016/j.orgel.2010.01.006.
- 32 S. Rajasekar and N. Hari, Synthesis and Polymerization of Benzoxazine Molecules with Electron-Withdrawing Group Substitution and Ring-Opening Polymerization, *High Perform. Polym.*, 2016, **29**(3), 349–361, DOI: 10.1177/0954008316644970.
- 33 S. Kowarik, A. Gerlach, S. Sellner, F. Schreiber, L. Cavalcanti and O. Konovalov, Real-Time Observation of Structural and Orientational Transitions during Growth of Organic Thin Films, *Phys. Rev. Lett.*, 2006, **96**(12), 125504, DOI: 10.1103/PhysRevLett.96.125504.
- 34 F. Schreiber, Organic Molecular Beam Deposition: Growth Studies beyond the First Monolayer, *Phys. Status Solidi A*, 2004, 1037–1054, DOI: 10.1002/pssa.200404334.
- 35 S. Kowarik, A. Gerlach and F. Schreiber, Organic Molecular Beam Deposition: Fundamentals, Growth Dynamics, Andin Situstudies, *J. Phys.: Condens. Matter*, 2008, **20**(18), 184005, DOI: 10.1088/0953-8984/20/18/184005.
- 36 L. Zhang, S. S. Roy, N. S. Safron, M. J. Shearer, R. M. Jacobberger, V. Saraswat, R. J. Hamers, M. S. Arnold and T. L. Andrew, Orientation Control of Selected Organic Semiconductor Crystals Achieved by Monolayer Graphene Templates, *Adv. Mater. Interfaces*, 2016, **3**(22), 1600621, DOI: 10.1002/admi.201600621.
- 37 J. Hagara, N. Mrkyvkova, P. Nádaždy, M. Hodas, M. Bodík, M. Jergel, E. Majková, K. Tokár, P. Hutár and M. Sojková, *et al.*, Reorientation of π -Conjugated Molecules on Few-Layer MoS₂ Films, *Phys. Chem. Chem. Phys.*, 2020, **22**(5), 3097–3104, DOI: 10.1039/C9CP05728E.
- 38 C. Schünemann, D. Wynands, K. J. Eichhorn, M. Stamm, K. Leo and M. Riede, Evaluation and Control of the Orientation of Small Molecules for Strongly Absorbing Organic Thin Films, *J. Phys. Chem. C*, 2013, **117**(22), 11600–11609, DOI: 10.1021/jp400604j.
- 39 H. Peisert, T. Schwieger, J. M. Auerhammer, M. Knupfer, M. S. Golden, J. Fink, P. R. Bressler and M. Mast, Order on Disorder: Copper Phthalocyanine Thin Films on Technical Substrates, *J. Appl. Phys.*, 2001, **90**(1), 466–469, DOI: 10.1063/1.1375017.
- 40 D. Yokoyama, Molecular Orientation in Small-Molecule Organic Light-Emitting Diodes, *J. Mater. Chem.*, 2011, **21**(48), 19187–19202, DOI: 10.1039/C1JM13417E.
- 41 C. H. Cheng, J. Wang, G. T. Du, S. H. Shi, Z. J. Du, Z. Q. Fan, J. M. Bian and M. S. Wang, Organic Solar Cells with Remarkable Enhanced Efficiency by Using a CuI Buffer to Control the Molecular Orientation and Modify the Anode, *Appl. Phys. Lett.*, 2010, **97**(8), 83305, DOI: 10.1063/1.3483159.
- 42 G. Duva, A. Mann, L. Pithan, P. Beyer, J. Hagenlocher, A. Gerlach, A. Hinderhofer and F. Schreiber, Template-Free Orientation Selection of Rod-Like Molecular Semiconductors in Polycrystalline Films, *J. Phys. Chem. Lett.*, 2019, **10**(5), 1031–1036, DOI: 10.1021/acs.jpclett.9b00304.
- 43 A. Winkler, On the Nucleation and Initial Film Growth of Rod-like Organic Molecules, *Surf. Sci.*, 2016, **652**, 367–377, DOI: 10.1016/j.susc.2016.02.015.
- 44 N. Mrkyvkova, M. Hodas, J. Hagara, P. Nadazdy, Y. Halahovets, M. Bodik, K. Tokar, J. W. Chai, S. J. Wang and D. Z. Chi, *et al.*, Diindenoperylene Thin-Film Structure on MoS₂ Monolayer, *Appl. Phys. Lett.*, 2019, **114**(25), 251906, DOI: 10.1063/1.5100282.
- 45 A. Operamolla and G. M. Farinola, Molecular and Supramolecular Architectures of Organic Semiconductors for Field-Effect Transistor Devices and Sensors: A Synthetic Chemical Perspective, *Eur. J. Org. Chem.*, 2011, **2011**(3), 423–450, DOI: 10.1002/ejoc.201001103.
- 46 J. Zaumseil and H. Sirringhaus, Electron and Ambipolar Transport in Organic Field-Effect Transistors, *Chem. Rev.*, 2007, **107**(4), 1296–1323, DOI: 10.1021/cr0501543.
- 47 M. Sojková, P. Siffalovic, O. Babchenko, G. Vanko, E. Dobročka, J. Hagara, N. Mrkyvkova, E. Majková, T. Ižák and A. Kromka, *et al.*, Carbide-Free One-Zone Sulfurization Method Grows Thin MoS₂ Layers on Polycrystalline CVD Diamond, *Sci. Rep.*, 2019, **9**(1), 2001, DOI: 10.1038/s41598-018-38472-9.
- 48 S. R. Forrest, Ultrathin Organic Films Grown by Organic Molecular Beam Deposition and Related Techniques, *Chem. Rev.*, 1997, **97**(6), 1793–1896, DOI: 10.1021/cr941014o.
- 49 K. A. Ritley, B. Krause, F. Schreiber and H. Dosch, A Portable Ultrahigh Vacuum Organic Molecular Beam Deposition System for in Situ X-Ray Diffraction Measurements, *Rev. Sci. Instrum.*, 2001, **72**(2), 1453–1457, DOI: 10.1063/1.1336822.
- 50 R. Hayakawa, A. Turak, X. Zhang, N. Hiroshiba, H. Dosch, T. Chikyow and Y. Wakayama, Strain-Effect for Controlled Growth Mode and Well-Ordered Structure of Quaterylene Thin Films, *J. Chem. Phys.*, 2010, **133**, 034706, DOI: 10.1063/1.3456733.
- 51 S. Kowarik, A. Gerlach, S. Sellner, L. Cavalcanti, O. Konovalov and F. Schreiber, Real-Time X-Ray Diffraction Measurements of Structural Dynamics and Polymorphism in Diindenoperylene Growth, *Appl. Phys. A: Mater. Sci. Process.*, 2009, **95**, 233–239, DOI: 10.1007/s00339-008-5012-2.
- 52 N. Mrkyvkova, *et al.*, Simultaneous Monitoring of Molecular Thin Film Morphology and Crystal Structure by X-Ray Scattering, *Cryst. Growth Des.*, 2020, **20**(8), 5269–5276, DOI: 10.1021/acs.cgd.0c00448.
- 53 K. Oura, M. Katayama, A. V. Zotov, V. G. Lifshits and A. A. Saranin, *Growth of Thin Films*, Springer, Berlin, Heidelberg, 2003, DOI: 10.1007/978-3-662-05179-5_14.
- 54 A. C. Dürr, F. Schreiber, M. Münch, N. Karl, B. Krause, V. Kruppa and H. Dosch, High Structural Order in Thin Films of the Organic Semiconductor Diindenoperylene, *Appl. Phys. Lett.*, 2002, **81**(12), 2276–2278, DOI: 10.1063/1.1508436.
- 55 A. E. Lauritzen, M. Torkkeli, O. Bikondoa, J. Linnet, L. Tavares, J. Kjelstrup-hansen and M. Knaapila, Structural

- Evaluation of 5,5'-Bis(Naphth-2-yl)-2,2'-Bithiophene in Organic Field-Effect Transistors with N-Octadecyltrichlorosilane Coated SiO₂ Gate Dielectric, *Langmuir*, 2018, **34**(23), 6727–6736, DOI: 10.1021/acs.langmuir.8b00972.
- 56 U. Heinemeyer, R. Scholz, L. Gisslén, M. I. Alonso, J. O. Ossó, M. Garriga, A. Hinderhofer, M. Kytka, S. Kowarik and A. Gerlach, *et al.*, Exciton-Phonon Coupling in Diindenoperylene Thin Films, *Phys. Rev. B: Condens. Matter Mater. Phys.*, 2008, **78**(8), 85210, DOI: 10.1103/PhysRevB.78.085210.
- 57 M. Sojková, K. Vegso, N. Mrkyvkova, J. Hagara, P. Hutár, A. Rosová, M. Čaplovičová, U. Ludacka, V. Skákalová and E. Majková, *et al.*, Tuning the Orientation of Few-Layer MoS₂ Films Using One-Zone Sulfurization, *RSC Adv.*, 2019, **9**, 29645, DOI: 10.1039/C9RA06770A.
- 58 M. Hodas, P. Siffalovic, P. Nádaždy, N. Mrkyvková, M. Bodík, Y. Halahovets, G. Duva, B. Reisz, O. Konovalov and W. Ohm, *et al.*, Real-Time Monitoring of Growth and Orientational Alignment of pentacene on Epitaxial Graphene for Organic Electronics, *ACS Appl. Nano Mater.*, 2018, **1**(6), 2819–2826, DOI: 10.1021/acsanm.8b00473.